Available online at www.eccomasproceedia.org
Eccomas Proceedia COMPDYN (2023) 544-559

ECCOMAS
Proceedia

COMPDYN 2023
9th ECCOMAS Thematic Conference on
Computational Methods in Structural Dynamics and Earthquake Engineering
M. Papadrakakis, M. Fragiadakis (eds.)
Athens, Greece, 12-14 June 2023

ASSESSING THE PERFORMANCE OF EXISTING RC BEAM-COLUMN JOINTS.

Emmanouil Golias[1], Demitrios Cotsovos[2]

[1]Dr. Civil Engineer
Democritus University of Thrace, Department of Civil Engineering,
Division of Structural Engineering, Xanthi 67100, GREECE
e-mail: egkolias@civil.duth.gr

[2]Associate Professor
Heriot Watt University,
Institute and Society, Institute for Infrastructure & Environment, United Kingdom
e-mail: d.cotsovos@hw.ac.uk

Abstract

The work presented herein sets out to study the behaviour of external beam-column joints with different reinforcement configurations that form part of existing RC structures and are often not been designed in accordance with current code provisions. The work is concerned with a numerical investigation of the behaviour of reinforced-concrete beam–column sub-assemblages under monotonic loading to assess the effect of crack-formation within the joint region on the overall response of the structural configurations considered. The behaviour of the latter specimens is investigated numerically using a nonlinear finite element analysis package (ADINA) which is capable of realistically accounting for the nonlinear behaviour of concrete and steel. The predictions of the numerical models developed are initially validated against published test data. The validated models are subsequently employed to provide insight into the mechanics underlying specimen behaviour as they approach their ultimate limit state. Each specimen is modelled twice, once with their joint region being modelled as a reinforced concrete member and then (a second time) with the joint region being assigned elastic properties. In most cases studies presented, the joints were found to suffer considerable cracking that initiated at early load stages. This led to an increase of the overall displacement values which was dependent however, on the configuration of the reinforcement provided. This indicates that the assumption of 'rigid joint', which is essentially implicit in methods used for the practical analysis of frames, is not always applicable when employed for the analysis of concrete structures.

Keywords: reinforced concrete, joints, nonlinear analysis, finite elements, design, failure

Peer-review under responsibility of the organizing committee of COMPDYN 2023.
doi: 10.7712/120123.10419.20844

1. Introduction

Practical structural analysis of reinforced concrete (RC) frames often adopts the assumption that the joint-regions behave essentially as rigid bodies. Therefore, the displacements and rotations are directly transferred through the joints to the ends of the intersecting one-dimensional (beam/column) members. For the case of RC structures, the ''rigid joint'' assumption is rather crude, since concrete behaviour is characterised by a low tensile strength and therefore, may exhibit cracking in the joint region even when subjected to levels of loading significantly lower than its load-carrying capacity. As a result, the displacements and rotations transferred through a joint to the ends of the adjacent one-dimensional elements may be affected by the cracking of the joint itself which in turn can affect the overall behaviour exhibited by the RC frame structure (to which it is a part of). This is not easily accounted for by the finite-element analyses packages used in practice for design purposes which employ linear (one-dimensional) beam/column elements. This shortcoming has been recognised in recent years and although there have been attempts to develop models that account for joint deformation [1-4] none of these models appear to be suitable for general application in practical structural analysis and design.

Current codes of practice employed particularly for the design of earthquake-resistant structures, specify design rules intended to ensure that joints remain essentially elastic (free of any significant cracking) while the adjoining beams experience plastic hinge formation due to the design actions [5–8]. Elastic joint deformation is considered sufficiently small allowing for the assumption of ''rigid joint'' to be assumed valid. In spite the considerable amount of research carried out to date on the behaviour of RC beam–column joints, the amount of transverse reinforcement specified by current codes of practice for the joint regions exhibits significant discrepancies, with the amount specified by EC8 [8] and ACI318 [6] being in many cases significantly different [9]. Furthermore, beam–column joint specimens designed in compliance with the earthquake-resistant design provisions of EC8 [8] have been reported to be unable to satisfy the code performance requirements, in that, not only do they exhibit considerable cracking in the joint region prior to plastic hinge formation in the adjacent beams, but, also, such cracking may occur at low levels of loading [10–13].

In view of the above, present work is intended to investigate numerically the effect of crack-formation within the joint region on the overall behaviour of a series of RC beam-column sub-assemblies characterised by different arrangements of reinforcement. The work makes use of ADINA [14] a non-linear finite-element analysis package which is capable of yielding realistic predictions concerning the behavior of a range of structural concrete configurations under different loading conditions. The behaviour of the beam/column sub-assemblages considered herein has been established experimentally in the past under static cyclic loading [15]. To investigate numerically the effect of crack-formation within the joint regions on the overall response of each RC beam/column sub-assemblage, the joints are first modelled as reinforced concrete structural elements (and therefore are allowed to crack) and then are assumed to behave elastically (thus not permitting the development of cracking within the joint region).

2. Beam – Column Joints Mechanisms of Load Transfer

The development of most models proposed to date for the design of beam-column joints is based on assumed mechanisms that describe how the joints resist the action of the forces transferred to them via the adjacent beam-column elements. The most common of such mechanisms are the diagonal strut (see Fig. 1a) and the truss (see Fig.1b) mechanism which, at the ultimate limit state (ULS), are usually assumed to act concurrently [16-20]. The diagonal strut is considered to resist the combined action of the normal and shear forces transferred to the joint through its interface with the compressive zone of the beam and column elements, whereas the truss resists the action of the bond forces developing at the interface between concrete and the portion of the longitudinal beam and column reinforcement anchored within the joint.

The above mechanisms have also been implicitly adopted by the current European codes [7, 8] which specify means for safeguarding against shear failure of the joint occurring before the formation of a plastic hinge in the region of the beam adjacent to it. The code specifications include the permissible value of the shear force at the joint mid-height, the anchorage length of the beam and column longitudinal steel bars and the amount and arrangement of transverse reinforcement of the joint. It is worth noting that the application of the Eurocode provisions for the design of earthquake-resistant joints has been found to lead to reinforcement congestion as well as design solutions that may not satisfy the code performance requirements [11-13, 21]. Attempts to improve the available design solutions have been primarily focused on either the derivation of a more refined analytical description of the stress conditions often accompanied by the implementation of modified versions of, the mechanisms mentioned earlier.

In an attempt to identify the causes of the observed behavior of beam-column joints, it was shown experimentally that the bond between concrete and the portion of the members' flexural reinforcement anchored within the joint has an insignificant effect on both the crack patterns and the strength of the joint. Moreover, it is realistic to expect that yielding of the flexural reinforcement of the beam and column members causes bond failure which extends deep into the joint where the reinforcement is anchored and, as a result, the largest part of the tensile forces sustained by the reinforcement is directly transferred at the opposite side of the joint as indicated in Fig. 2 (obtained from [9]). Such behavior precludes the development of a truss mechanism and thus it is only through the diagonal strut mechanism that the joint resists the action of the forces transferred to it from the adjacent beam and column members [22] as suggested in the early 1980s [23].

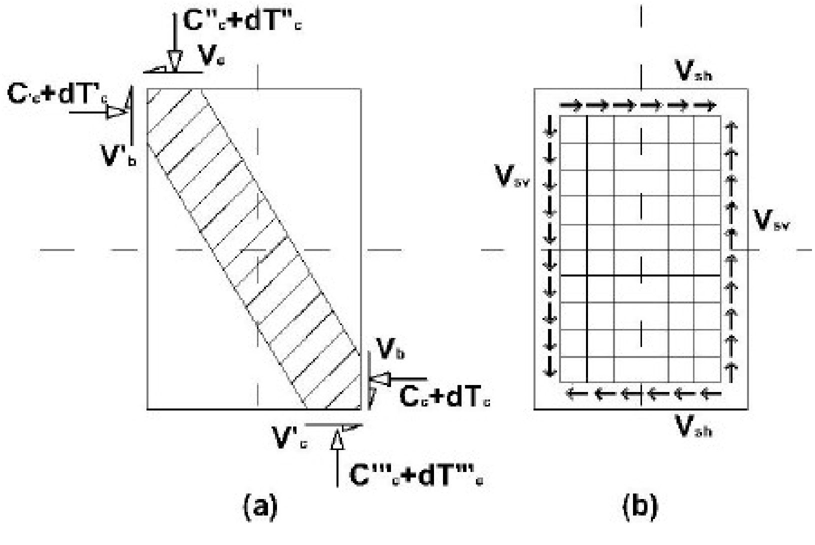

Figure 1: Schematic representations of (a) diagonal strut and (b) truss mechanisms of joint resistance [in (a): C_c, C_c', C_c'' and C_c''' are the compressive forces in concrete; C_s, C_s', C_s'' and C_s''' are the compressive forces in steel; and V_b, V_b', V_c, V_c' are the shear forces with subscripts b and c indicating the interfaces with beam and column, respectively. In (b): V_{sh} and V_{sv} the bond forces at the concrete-longitudinal steel of the beam-joint and column-joint interfaces, respectively]. [9]

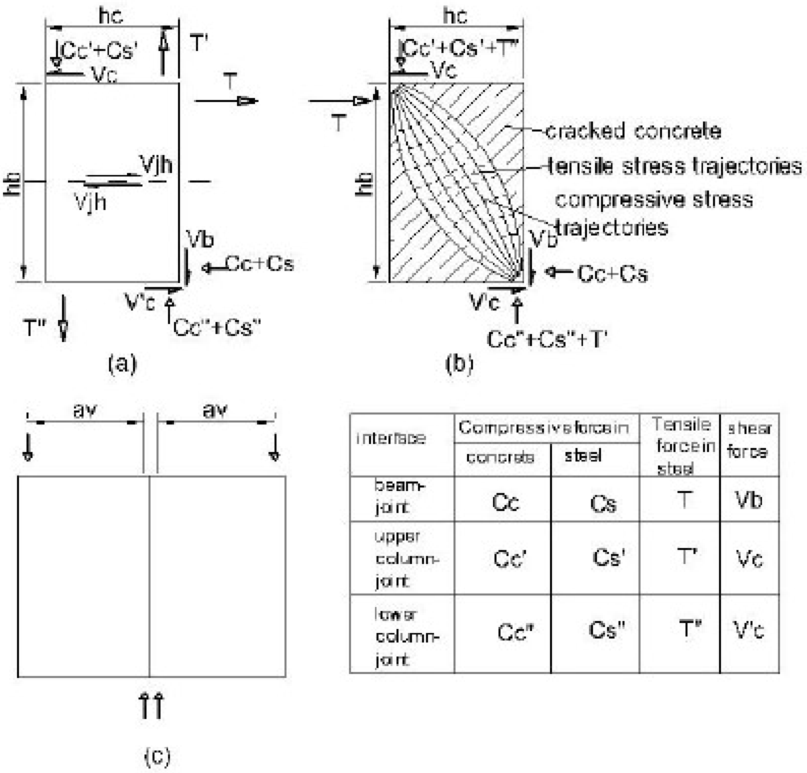

interface	Compressive forces in		Tensile force in steel	shear force
	concrete	steel		
beam-joint	Cc	Cs	T	Vb
upper column-joint	Cc'	Cs'	T'	Vc
lower column-joint	Cc"	Cs"	T"	V'c

Figure 2: (a) Forces acting at the interfaces of the joint with the beam and column elements and shear force Vjh at the horizontal cut at mid height of joint; (b) Compressive and tensile stresses trajectories assumed to develop within the joint at its ultimate limit state; and (c) Deep beam analogy. [9]

The flow of the compressive stresses between the upper and the lower diagonal ends of the joint is indicated by the compressive stress trajectories schematically represented in Fig. 2(b). The figure also shows the tensile stress trajectories which intersect at right angles those of the compressive stresses. It is the flow of the compressive stresses that forms the diagonal strut which is confined between the regions of the cracked concrete surrounding the portion of the members' flexural reinforcement anchored into the joint; such cracking occurs under the action of the tensile forces which are transferred from steel to concrete and eventually leads to loss of bond. [9]

3. Code requirements

The horizontal shear force (V_{jh}) acting at the joint mid height is obtained from $V_{jh} = T - V_c = 1.2A_{sl,b}f_y - V_c$ where $A_{sl,b}$ is the total area of the beam compressive longitudinal reinforcement, V_c is the value of the shear force at the upper column-joint interface corresponding to the formation of a plastic hinge at the beam-joint interface, and f_y the yield stress of the reinforcement.

When designing a RC exterior beam-column joint the acting shear force should be less than the joint strength, whereas an amount of transverse reinforcement should also be placed in the joint core. The expression used for calculating the joint strength calculation and the amount of the required transverse reinforcement differs in each code.

In the case of the Eurocodes [7, 8] $V_{jh} \leq V_{jR,h} = nf_{cd}\sqrt{(1 - v_d/n)}b_j h_{jc}$ where $n = 0.6(1 - f_{ck}/250)$, f_{cd} is the concrete design strength, $b_j = min\{b_c; (b_w + 0.5h_c)\}$ for $b_c > b_w$,or, $b_j = min\{b_w; (b_c + 0.5h_c)\}$ for$b_c < b_w$, (where b_c is column cross-sectional width, b_w the width of the beam web, and h_c the cross sectional column depth in the direction of interest), h_{jc} is the distance between extreme layers of column reinforcement. The total amount of transverse reinforcement is obtained for the following expressions:

$$A_{sh} \geq \left(\frac{\left(\frac{V_{jhd}}{b_j h_{jc}}\right)^2}{f_{ctm} + v_d f_{cd}} - f_{ctd} \right) \frac{b_j h_{jw}}{f_{yd}} \qquad A_{sh} \geq \frac{\gamma_{Rd} A_{s1} f_{yd}(1 - 0.8v_d)}{f_{yd}}$$

$A_{sh}$where A_{sh} is the total area of horizontal hoops, V_{jhd} is the design joint shear force, h_{jw} is the distance between the top and bottom beam reinforcement, and v_d is the normalized axial force of the column above.

In the case of ACI 318 [6] $V_{jh} \leq V_n = 20\sqrt{f_c} b_j h$ where $b_j$is the joint width; $b_j = b_c$ when $b_b \geq b_c$ or $b_j = (b_c + b_b)/2 \leq b_b + h_c/2$ when $b_b < b_c$ (where b_b and b_c are the widths of the beam and column, respectively), h is the height of the column cross section, and$f_c$is the concrete compressive strength ≤6000 psi (42MPa). The total cross-sectional area (in Imperial units) of the rectangular hoop reinforcement is obtained from the following expressions:

$$A_{sh} = 0.3\frac{s h_c f_c}{f_{yh}}\left({}^{A_g}\!/_{A_c} - 1\right) \qquad A_{sh} = 0.09\left(\frac{s h_c f_c}{f_{yh}}\right)$$

where s is the stirrup spacing,$h_c$is the height of the portion of the beam cross section enclosed by the stirrup center line,$f_{yh}$is the characteristic yield stress of the reinforcement, $A_g$is the gross column cross sectional area and A_c is the confined cross-sectional area.

It is worth noting that a number of alternative formulae have also been proposed to date [20, 22, 24] for determining the strength of the joint and the amount of reinforcement required. A summary of these alternative methods is provided elsewhere [9].

4. Case studies investigated.

Five (5) exterior beam-column sub-assemblages with different reinforcement configurations (mainly in the joint region) are investigated herein. The behaviour of these specimens has been established experimentally in the past under increasing levels of cyclic loading [15]. The design details of the specimens are presented in Fig. 3. The 28-day cylinder compressive strength of concrete was f_c=34 MPa whereas the steel of the longitudinal bars and the stirrups was f_y=550 MPa.

The experimental setup originally employed for testing the specimens considered is shown in Fig.3a. Each specimen was rotated 90° degrees with the columns being positioned horizontally and the beams vertically. The columns were supported on pins (which allowed rotation at the supports) representing the points of contraflexure located approximately at the middle of the columns in laterally loaded frame structures. During testing each column was initially subjected to a compressive axial force $N_c = 0.05 \cdot A_c \cdot f_c$ = 150 kN. Subsequently, all specimens where subjected to a horizontal concentrated load applied at the top end of the beam. The latter load was applied in the form load-cycles with increasing amplitudes. The sequence of the load cycles applied and the result obtained during testing are described elsewhere [15] .

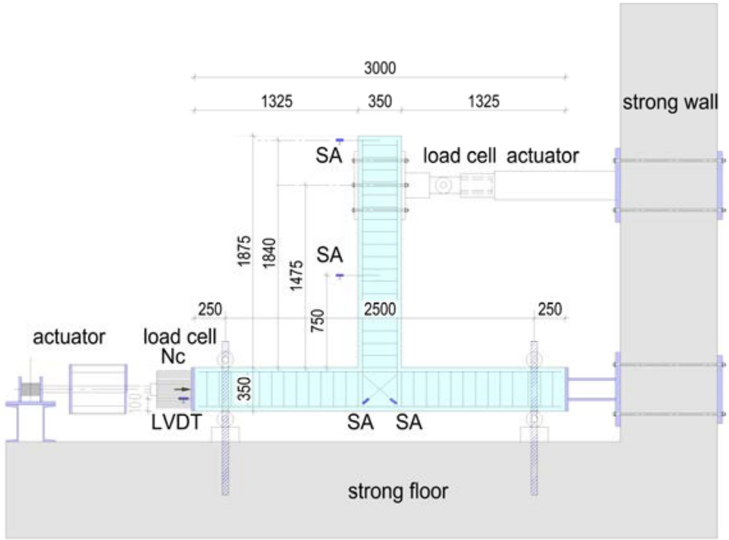

(a) Experimental setup originally employed for testing the specimens

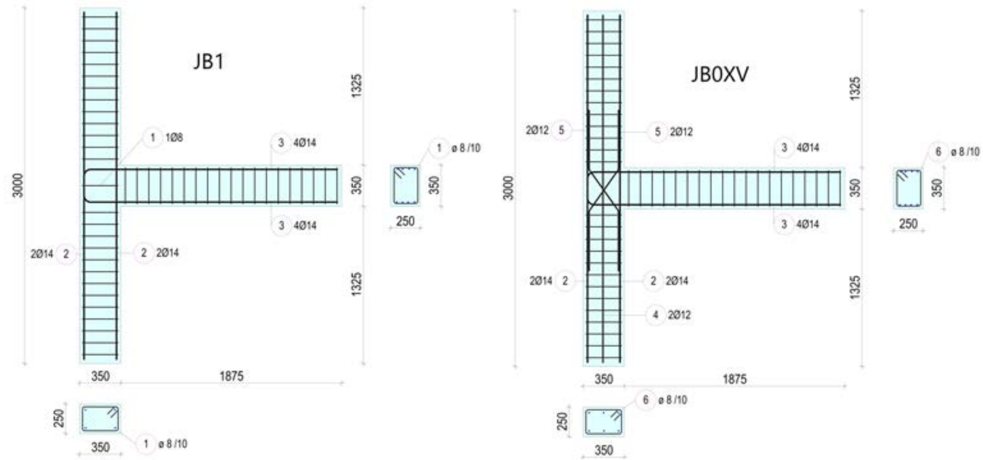

Reinforcements	Specimen JA1	Specimen JB0	Specimen JB1	Specimen JB1V	Specimen JB0VX
1	1Ø8	-	1Ø8	1Ø8	-
2	2Ø14	2Ø14	2Ø14	2Ø14	2Ø14
3	4Ø12	4Ø14	4Ø14	4Ø14	4Ø14
4	-	-	-	1Ø12	2Ø12
5	-	-	-	-	2Ø12

b) Design details of specimens considered

Figure 3: (a) Experimental setup originally employed during testing and (b) Design details of specimens considered [**15**]

The specimens considered are designated as JA1, JB0, JB1, JB1V and JB1VX [15] depending on the arrangement of the reinforcement provided (see Fig. 3b). The name of each specimen starts with the letter 'J' and is followed by a series of characters which describe its design characteristics. The letter 'J' was followed by the letter A or B depending on whether the beams were reinforced longitudinally by four (4) 12 mm or 14mm diameter bars respectively at the top and at the bottom of their cross-section. The third (numeric) character indicates the number of the stirrups (0 or 1) introduced in the body of the joint. Finally, the letter X was used when X-type reinforcement was introduced in the joint region whereas the letter V was used to indicate introduction of two extra 12mm diameter steel bars in the column cross-section as indicated in Fig. 3b.

5. FINITE ELEMNT MODELLING

Nonlinear finite element analysis is currently employed to complement the data established experimentally [15], gain more insight into mechanics underlying the behaviour (including the mode of failure) of the specimens exhibited during testing as well as the associated internal stress-state developing within the specimens as they approach the peak load. For this purpose, ADINA is employed which is capable of accounting for the nonlinear behaviour of concrete and steel and provide realistic predictions of RC structural response [14].

The experiment presented in the previous section is modelled as a 2D plain-stress problem. Concrete is modelled using a mesh of 9-noded elements with a 3x3 integration rule (see Fig. 4a) whereas the steel reinforcement bars are modelled using 2-node truss elements of appropriate cross-sectional area which are embedded within the finite element (FE) mesh representing the concrete medium (see Figs 4b-d).

The constitutive model employed by ADINA [15] to describe the behaviour of concrete stems from experimental data obtained from tests conducted on concrete cylinders under triaxial loading conditions and has been used in the past to predict the behaviour of a wide range of structural concrete configuration under different loading conditions [25]. Steel material behaviour is modelled via a simple biaxial model describing material behaviour under uniaxial compression and tension. Full bond is assumed between the steel rebar and concrete. The load is applied monotonically to failure in the form of displacement increments (displacement control) and the problem.

The Sparce method [14] is employed to solve the problem iteratively (during every load increment). Convergence is checked locally at each integration point. Once the values of the correction of the displacement (obtain from each iteration) becomes less than a small, predefined value (convergence criterion) the solution proceeds on the next load increment. The smeared-crack approach is adopted for modelling cracking. A crack is considered to form when the stress developing at a specific location of the structure corresponds to a point in the principal stress space that lies outside the predefined failure surface [16] adopted for the case of concrete. This is then followed by an abrupt loss of load-carrying capacity in the direction normal to the plane of the crack while at the same time, the shear stiffness is reduced to 10% of its previous value (before the occurrence of the crack). It is not set to zero to reduce the risk of numerical instability during the execution of the solution procedure.

As mentioned earlier, each specimen considered is investigated twice. Each joint of the beam-column sub-assemblages are first modelled as reinforced concrete structural elements (allowing crack-formation to occur in this region) and then is considered to behave elastically, thus not permitting the development of cracking within is region. The case studies caried out are named after the specimens mentioned earlier. When allowing cracking to develop within the joint regions the case studies carried out are designated as JA1, JB0, JB1, JB1V and JB1VX whereas when the joint is modelled elastically the corresponding case studies are designated as JA1-L, JB0-L, JB1-L, JB1V-L and JB1VX-L.

Finally, it is noted that although the behaviour of the specimens was originally established experimentally under cyclic loading, in the numerical studies the load is applied in the form of a static load which increases monotonically until failure of the specimen occurs.

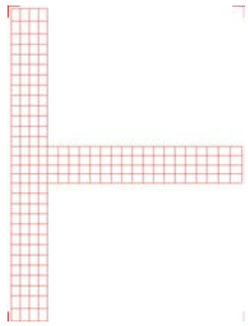

(a) FE mesh representing concrete

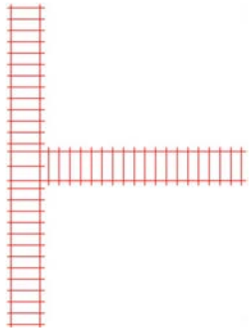

(b) FE mesh representing the reinforcement in JA1, JB1, JB1V

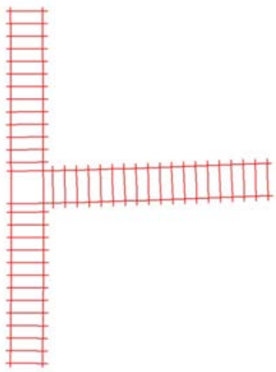

(c) FE mesh representing the reinforcement in JB0

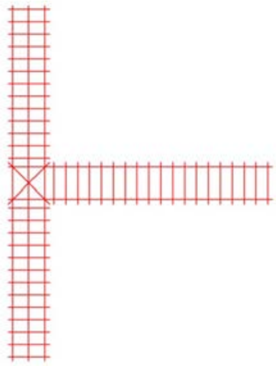

(d) FE mesh representing the reinforcement in JB1VX

Figure 4: Finite element mesh adopted for modelling (a) concrete and (b-d) the reinforcement of the specimens considered.

6. Validation of numerical predictions

The predictions obtained from ADINA concerning the behaviour of specimens in case studies JA1, JB0, JB1, JB1V and JB1VX are presented in Figs 5 to 9. The numerical predictions obtained are initially provided in the form of load-deflections curves. Attention is then focused on obtaining an understanding of the internal stress-state developing along the members of the structural configuration considered (and the joint region in particular) as they approach the peak load. This is achieved through the analysis of the predictions concerning (a) the crack patterns, (b) the distribution of the principial (compressive) stresses developing within the concrete as well as (c) the axial stresses developing along the reinforcement bars at peak loads. These predictions reveal the path followed by the load from the point of application to the supports and can be used as a guide the development of models capable of describing the behaviour of the specimen.

The predictions are presented in the form of:

(a) curves describing the variation of the applied load with the deflection exhibited at the load point for each case study considered (see Figs 5a to 9a). These curves are plotted against the envelop curves describing the hysteretic response of the specimens which were established experimentally in the past [15].

(b) The cack patterns predicted to develop at peak load. These are presented in Figs 5c to 9c for both case studies considered (once assuming that cracking was allowed to develop within the joint regions and a second time during which the joint region was considered to behave elastically. The predicted crack patterns are subsequently compared against their counterparts established experimentally [15] (see Figs 5b to 9b)

(c) Contour and vector plots (see Figs 5d to 9d) showing the distribution of the principial stresses developing at peak load along the components of the structural forms considered. The values of the maximum compressive stresses developing within the concrete as well as the location at which it is observed is also highlighted in Figs 5d to 9d.

(d) Plots showing the distribution of the axial stresses developing within the reinforcement of the specimens (see Figs 5e to 9e.). The values of the maximum compressive and tensile stresses developing along the reinforcement bars as well as the location at which these are exhibited are also highlighted.

The comparison between the numerically predicted load-deflection curves (established for the case of monotonic loading) obtained from case studies JA1, JB0, JB1, JB1V and JB1VX and the associated envelope curves [15] established experimentally (which describe the hysteretic response recorded during testing) are presented in Fig.5a to 9a reveals good agreement between the two set of data. The fact that the numerically predicted values of peak load are somewhat higher than those established experimentally is likely to be attributed to the fact that in the numerical investigation the load was applied monotonically to failure and not in the form of load cycles. The crack patterns predicted numerically (see Figs 5c to 9c) appear also in agreement to those established experimentally (see Figs 5b to 9b).

The distribution of the principal stresses clearly demonstrates that the behaviour of joints is dominated by compressive stresses and the development of an inclined strut. In the case of specimens JA0 and JA1VX the max value of the compressive stress developing in the concrete is located in the compressive zone of the beam in the area adjacent to the joint. Reviewing the axial stresses predicted to develop along the reinforcement bars, it is observed that no yielding of reinforcement occurs within the joint region which suggest that the cracking developed is not extensive. This is compatible with the behaviour established during the testing of specimens JA0 and JA1VX. Both specimens exhibited low levels of cracking in the joint region and significant flexural cracking in the beam which is a clear indicator of plastic hinge formation. In the case of specimens JB0, JB1, JB1V the maximum value of compressive stress develops within the joint region. Reviewing the axial stresses predicted to develop along the reinforcement bars it can be seen that the reinforcement within the join region yields. This is in line with the experimentally established behaviour of specimens JB0, JB1, JB1V where a significant level of cracking was observed in the joint region.

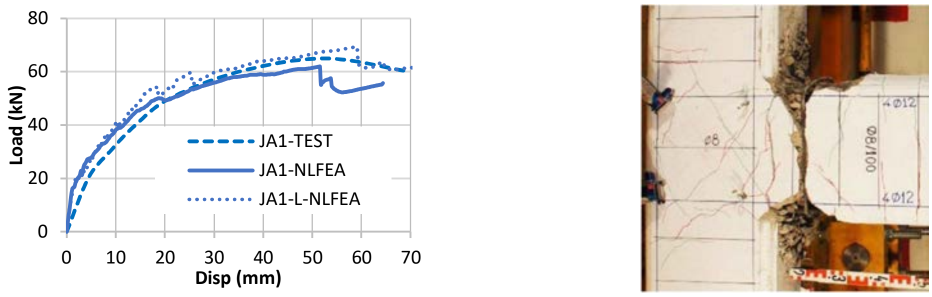

(a) Load deflection curves (b) Cracking recorded during testing

JA1 (Concrete joint) JA1-L (Rigid joint)

(c) cracking at peak load

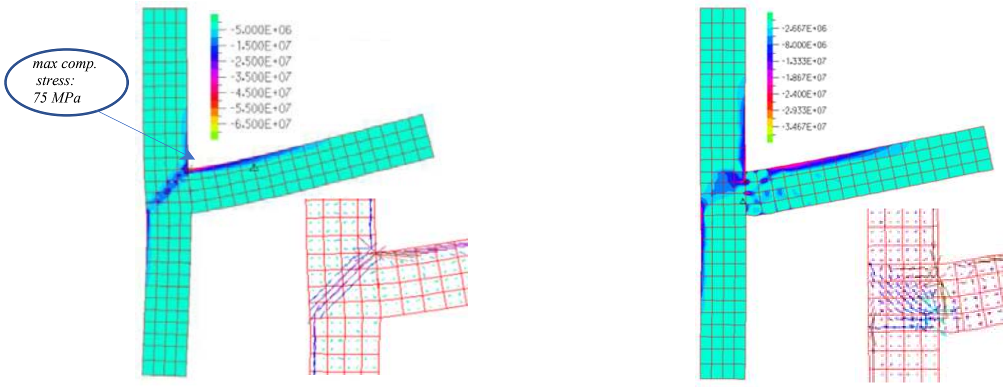

JA1 (Concrete joint) JA1-L (Rigid joint)

(d) Distribution of principal stresses (presented as contours and vectors)

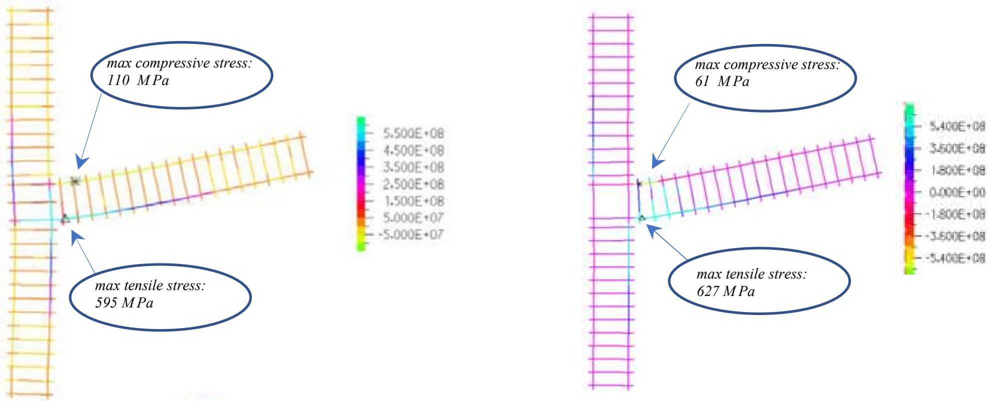

JA1 (Concrete joint) JA1-L (Rigid joint)

(e) Axial stress developing within the reinforcement bars

Figure 5: Predictions obtained from case studies JA1 and JA1-L

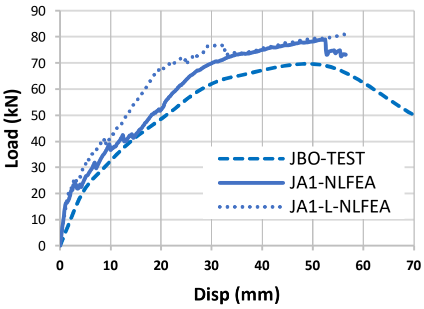

(a) Load deflection curves

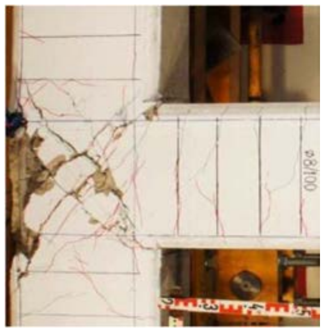

(b) Cracking recorded during testing

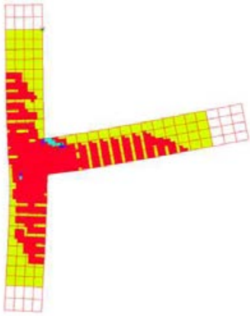

JB0 (Concrete joint)

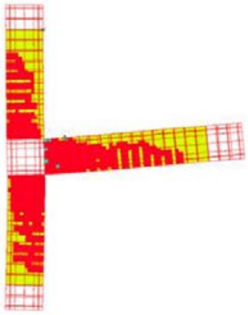

JB0-L (Rigid joint)

(c) cracking at peak load

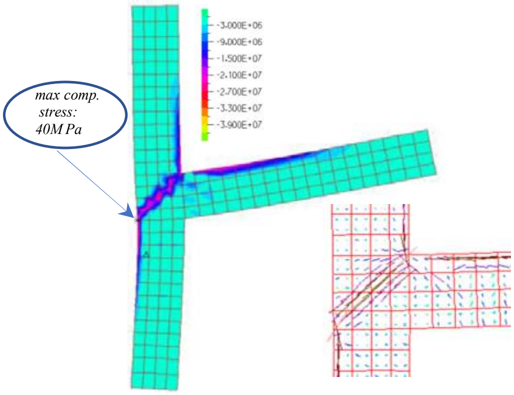

JB0 (Concrete joint)

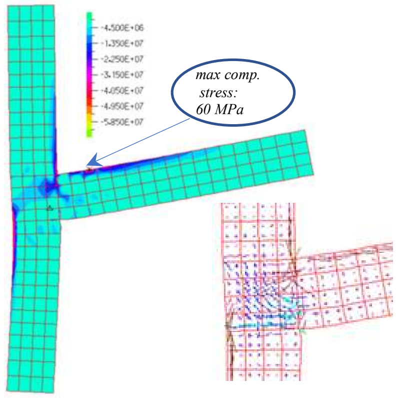

JB0-L (Rigid joint)

(d) Distribution of principal stresses (presented as contours and vectors)

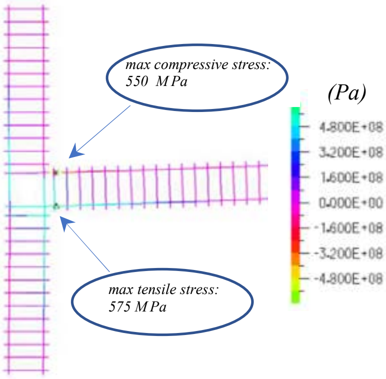

JB0 (Concrete joint)

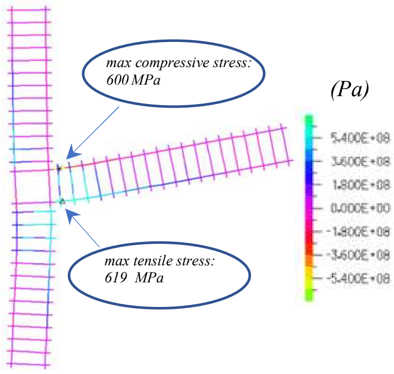

JB0-L (Rigid joint)

(e) Axial stress developing within the reinforcement bars

Figure 6: Predictions obtained from case studies JB0 and JB0-L

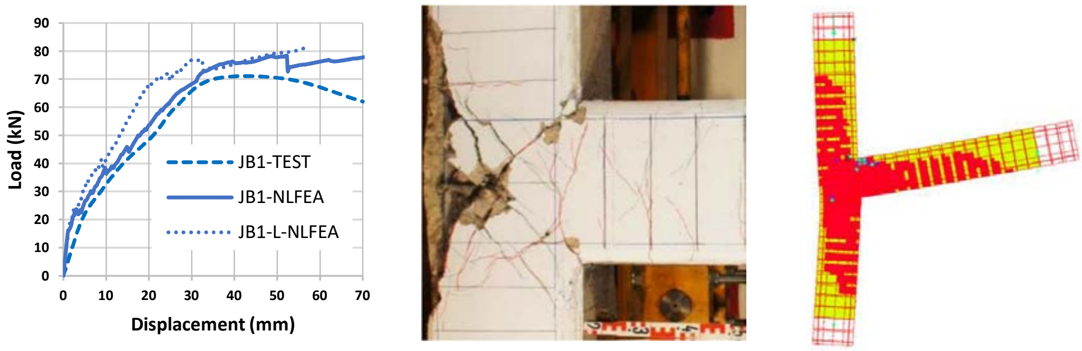

(a) Load deflection curves (b) Cracking during testing (c) cracking at peak load

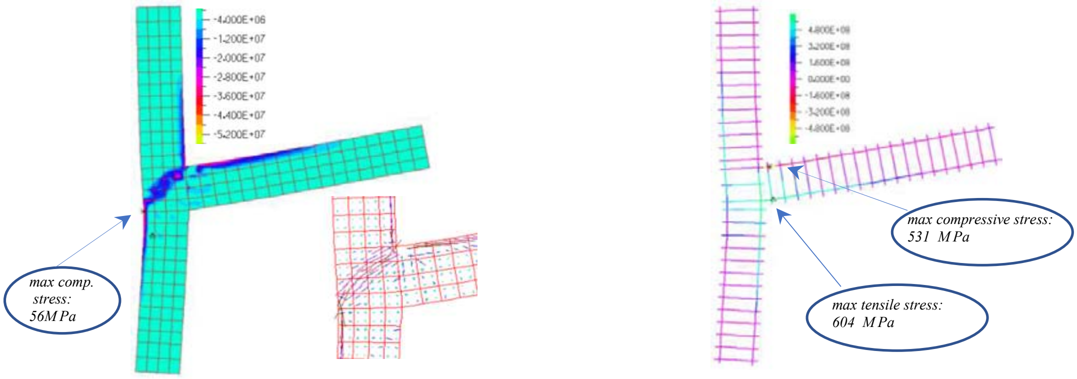

(d) Distribution of principal stresses (e) Axial stress along the reinforcement bars

Figure 7: Predictions obtained from case studies JB1 and JB1-L (it is noted that the behaviour of JB1-L is identical to that of JB0-L)

(a) Load deflection curves (b) Cracking during testing (c) cracking at peak load

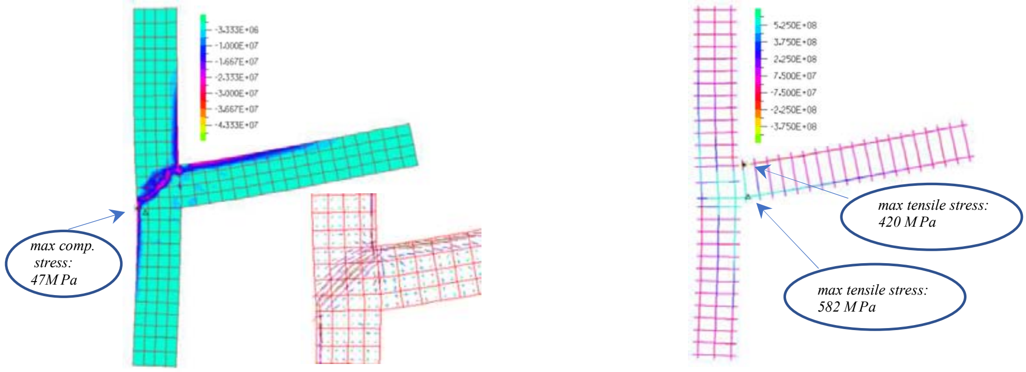

(d) Distribution of principal stresses (e) Axial stress along the reinforcement bars

Figure 8: Predictions obtained from case studies JB1V and JB1V-L. (it is noted that the behaviour of JB1V-L is identical to that of JB0-L)

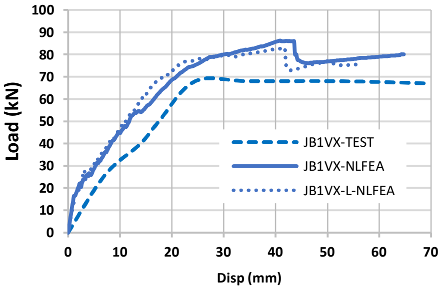

(a) Load deflection curves

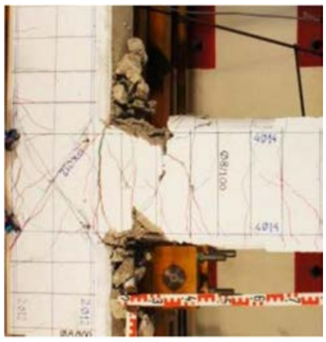

(b) Cracking recorded during testing

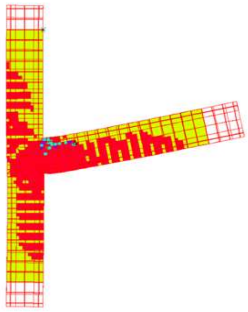

JB1VX (Concrete joint)

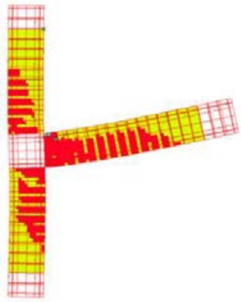

JB1VX (Concrete joint)

(c) cracking at peak load

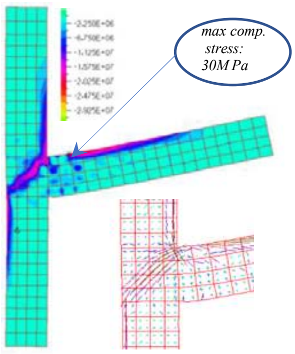

JB1VX (Concrete joint)

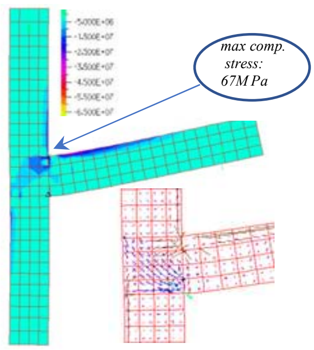

JB1VX -L (Rigid joint)

(d) Distribution of principal stresses (presented as contours and vectors)

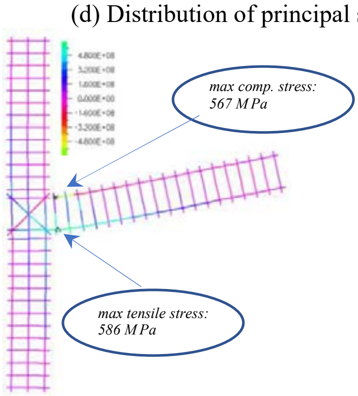

JB1VX (Concrete joint)

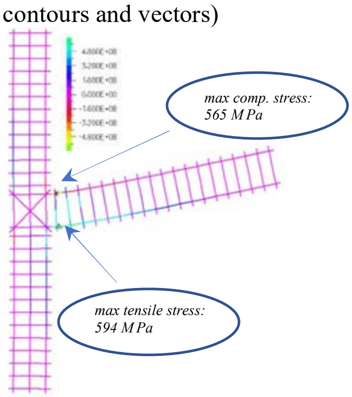

JB1VX -L (Rigid joint)

(e) Axial stress developing within the reinforcement bars

Figure 9: Predictions obtained from case studies JB1VX and JB1VX-L

7. Investigating the effect of cacking within the joint region.

Comparing the predictions obtained from the case studies where crack-formation was allowed to develop within the joint to those obtained from the case studies where elastic material properties were assigned to the joint region, it can be seen that the effect of crack formation is more prominent in the case of specimens JB0, JB1, JB1V and to a lesser extent on specimens JA1 and JB1VX. Comparing the load deflection curves obtained for case studies JB0, JB1 and JB1V with those obtained from case study JB0-L, JB1-L and JB1V-L respectively, it can be seen that although there is not much difference in terms of specimen load-carrying capacity, the displacement predicted with increasing levels of loading is larger when cracking is allowed within the joint region. This indicates that cracking within the joint region can cause a more rapid reduction/deterioration of the stiffness of the structure as loading increases. Comparing the load deflection curves obtained for case studies JA1 and JB1VX it is evident that the predictions obtained when allowing for crack formation in the joint region are similar to those obtained when assigning elastic properties to the joint region. This suggest that that the designs adopted for the two latter specimens can successfully safeguard against significant crack formation in the joint region thus indicating that the application of the 'rigid joint', in these cases, is valid.

8. Conclusions

The finite element models developed were able to provide realistic predictions of the behavior of the beam-column sub-assemblages considered. The predictions obtained appear to be in generally good agreement with the revenant test data. The numerical analysis demonstrated that when allowing cracks to form within the joint region this can have significant effect on the overall structural behaviour of the specimens considered. The extent of this effect however, depends on the layout of the reinforcement introduced in the joint region as well as the flexural capacity of the columns relative to that of the beam connected to the joint. In the case of specimens JA1 and JB1VX the predictions obtained when allowing cracks to open in the joint region were very similar to those obtained when adopting the rigid joint assumption. As a result, practical structural analysis, based on the assumption of rigid joints, yields results that can safeguard the code specified margins of safety and structural performance requirements when certain conditions concerning the design of the specimens are met. In view of the above, it appears that there is an urgent need for improving current design methods so as to allow for the inconsistencies resulting from the condition for rigid joint behaviour that underlies current methods for frame analysis.

9. References

[1] El-Metwally S, Chen WF. Moment-rotation modelling of reinforced concrete beam–column connections. ACI Struct J 1988;85(4):384–94.

[2] Ghobarah A, Biddah A. Dynamic analysis of reinforced concrete frames including joint shear deformation. Eng Struct 1999;21(11):971‐87.

[3] Anderson M, Lehman D, Stanton J. A cyclic shear stress‐strain model for joints without transverse reinforcement. Eng Struct 2007;30(4):941‐54.

[4] Birely AC, Lowes LN, Lehmam DE. A model for the practical nonlinear analysis of reinforced-concrete frames. Eng Struct 2012;34(4):455‐65.

[5] Architectural Institute of Japan. Design guidelines for earthquake resistant reinforced concrete buildings based on inelastic displacement concept. Tokyo: AIJ; 1999. 440 pp [in Japanese].

[6] American Concrete Institute. Building code requirements for structural concrete (ACI 318-02) and commentary (ACI 318R-02); 2002.

[7] EN 1992-1. Eurocode 2 (EC2): design of concrete structures. Part 1-1: general rules and rules for buildings; 2004.

[8] EN 1998-1. Eurocode 8 (EC8): design of structures for earthquake resistance. Part 1: general rules, seismic actions and rules for buildings; 2004.

[9] Kotsovou M.G, Kotsovos M.D. Improving the design of earthquake resistant reinforced concrete exterior beam-column joints. The structural Engineer 2013.

[10] Ehsani MR, Wight JK. Effect of transverse beams and slab on behaviour of reinforced concrete beam-to-column connections. ACI J 1985;82(2):188–95.

[11] Ehsani MR, Wight JK. Exterior reinforced concrete beam-to-column connections subjected to earthquake-type loading. ACI J 1985;82(4):492–9.

[12] Tsonos AG, Tegos IA, Penelis GG. Seismic resistance of type 2 exterior beam– column joints with inclined bars. ACI Struct J 1992;89(1):3–12.

[13] Hwang Shyh-Jiann, Lee Hung-Jen, Liao Ti-Fa, Wang Kuo-Chou, Tsai Hsin-Hung. Role of hoops on shear strength of reinforced concrete beam–column joints. ACI Struct J 2005;102(3):445–53.

[14] Available: https://www.adina.com

[15] Karayannis C.G, Golias E. Full scale tests of RC joints with minor to moderate seismic damage reaired using C-FRP sheets. Earthquake and Structures 2018;15(6): 617-618.

[16] Paulay, T., Park, R., and Priestey, M. J. N., “Reinforced Concrete Beam – Column Joints Under Seismic Actions,” ACI Journal, 1978, 75(11): 585-593.

[17] Paulay, T., “Equilibrium Criteria for Reinforced Concrete Beam – Column Joints,” ACI Structural Journal, 1989, 86(6): 635-643.

[18] Leon, R. T., “Shear Strength and Hysteric Behaviour of Interior Beam – Column Joints,” ACI Structural Journal, 1990, 87(1):3-11.

[19] Paulay, T., and Priestley, M. J. N., Seismic Design of Reinforced Concrete and Masonry Buildings. J. Willey & Sons, New York, 1992.

[20] Tsonos, A. G., “Cyclic load behaviour of reinforced concrete beam – column subassemblages designed according to modern codes,” European Earthquake Engineering, 2006, 3: 3-21.

[21] Kotsovou GM, Mouzakis H. Seismic behaviour of RC external joints. Mag Concr. Res 2011;33(4):247–64.

[22] Kotsovou G, Mouzakis H. Seismic design of RC external beam-column joints. Bull Earthquake Eng 2012;10(2):645–77.

[23] Zhang, L., and Jirsa, J.O., A study of the shear behaviour of reinforced concrete beam-column joints. RMFSEL Report No. 82-1, Phil. M. Ferguson Structural Engineering Laboratory, University of Texas at Austin, Feb. 1982.

[24] Vollum R.L. and Newman J.B. Strut and tie models for analysis/design of external beam-column joints. Magazine of Concrete Research, 1999, 51(6): 415-425

[25] Kotsovos M.D., Finite-Element Modelling of Structural Concrete: Short-Term Static and Dynamic Loading Condition, CRC Press, 2015.